Intelligent Control and System Engineering 2023; 1(1): 367.
Original Research Article

Improved generalized self-consistent model in predicting the applicability of the refractory material mechanics behavior research

Zhixing Huang, Zhigang Wang*, Xianjun Li, Jiawen Li, Tianyang Zhou, Dongshuo Wang

School of Mechanical Automation, Wuhan University of Science and Technology, Wuhan 430081, Hubei Province, China

*** Corresponding author:** Zhigang Wang, 35067795@qq.com

ARTICLE INFO

Received: 24 December 2023
Accepted: 26 December 2023
Available online: 4 February 2024

doi: 10.59400/icse.v1i1.367

ABSTRACT: The improved generalized self-consistent model (GSCM) has shown good performance in predicting the mechanical properties of multiphase refractory materials. In this study, three representative refractory materials were selected to investigate the applicability of this model. Under ambient conditions, the mechanical properties of aluminum-magnesium-carbon material with multiple inclusions, magnesium-carbon material with low matrix and high aggregate content, and aluminum matrix material were predicted. The damage behavior of the materials under compression was simulated using an iterative method. The results showed that the GSCM still exhibited good predictive performance for the elastic modulus and Poisson's ratio of multiphase inclusion materials and aluminum matrix materials, with errors of approximately 5%. When simulating the compressed damage behavior, the maximum error for AMC-type materials was around 10%, while for aluminum matrix materials, it was around 25%. The maximum errors occurred near the maximum strain, which was attributed to the excessive pore conversion rate in the GSCM when simulating material damage. At non-maximum strains, the fitting error was within an acceptable range, achieving the purpose of estimating the mechanical properties of the materials using this model. However, the predictive performance for materials with low matrix and high aggregate content was poor due to the inherent characteristics of these materials, where the matrix cannot effectively encapsulate the aggregates, resulting in heterogeneous mechanical properties at the macroscopic level. The limitations of the GSCM mechanism prevented it from achieving accurate predictions in such cases. In conclusion, the generalized self-consistent model can be applied to estimate the mechanical properties of various composite materials. However, for materials with heterogeneous mechanical properties, such as those where the matrix cannot effectively encapsulate the particle phase, the GSCM is not suitable.

KEYWORDS: generalized self-consistent model; multiphase refractory materials; mechanical property prediction; damage behavior; iterative method

1. Introduction

Refractory materials work in complex working environments, such as high temperatures, high

pressure, and chemical corrosion. These conditions make the material prone to damage and cracks, which affect its service life and safety. Mechanical properties of the material are usually closely related to its microstructure[1], so domestic and foreign scholars from the perspective of micro[2–6] proposed many effective methods to predict the mechanical properties of materials, including the proper use of the generalized self-consistent model, which can accurately predict the material mechanical properties and can conform to the predicted volume change process of material damage.

Huang et al.[2] proposed an improved micro-scale Chamis model and a meso-scale stiffness averaging method with porosity defects to study the effect of porosity on three-dimensional composites. Schmitt et al.[3] used micromechanics to predict the mechanical properties of two aluminum-based ceramics and pointed out that the method was suitable for aluminum-carbon composites. Liu et al.[6] simulated the mechanical behavior of Mg-Carbon refractories under tensile and compressive conditions, combined with the generalized self-consistent model from the perspective of micromechanics, and simulated the mechanical properties and damage of the material. The results showed that the model was suitable for these two-phase Mg-Carbon refractories. Wang et al.[5] proposed an improved generalized self-consistent model based on the traditional two-phase generalized self-consistent model, combined with the weighted average method, and used this model to predict the properties of aluminum-carbon multiphase refractories. The results showed that the improved generalized self-consistent model performed well in predicting the properties of this multiphase material, greatly expanding the scope of application of the model. Lurie et al.[7] used the generalized self-consistent method to predict the mechanical properties of a three-phase composite fiber material, and the predicted results were completely consistent with the results of the multivariate statistical analysis method, which proved the advantages of the generalized self-consistent method in the analysis of composite material properties. This study further expands the research content on the basis of the above and selects three materials with different characteristics to investigate the applicability of the model.

Domestic and foreign scholars have conducted a lot of research on material properties from a microscopic perspective, involving a number of different types of research fields, in which the generalized self-consistent model, as a common means of research, has shown its advantages of simplicity and accuracy for a variety of refractories, but there are few discussions on the applicability of the improved generalized self-consistent model. Its scope of application is still unclear. As far as the current research is concerned, the main research object of scholars is carbon matrix refractories with the matrix volume fraction concentrated between 30% and 60%, and the prediction effect of this model for other types of refractories has not been determined. Three kinds of refractors—aluminum-magnesia carbonite with multiple inclusion phases, magnesia carbonite with low matrix and high aggregate, and aluminum-matrix materials—were selected to explore the applicability of the improved generalized self-consistent model to predict the properties of different types of materials and to simulate the damage of materials under tensile and compression conditions.

2. Improved generalized self-consistent model prediction

2.1. Generalized self-consistent model

There is a directly relationship between the behavior of refractory materials under mechanical, thermodynamic, and mechanical loading and the composition, particle size, purity, and content of the raw materials, all of which determine the microstructure and mechanical properties of the materials. The generalized self-consistent model is appropriate for the prediction of the properties of such

composites[2].

The rationale of the generalized self-consistent model is to embrace the inclusions and their enclosing medium into an equivalent homogeneous medium of infinite size with unknown properties, impose the corresponding boundary conditions at its boundaries, and obtain the equivalent properties of the composite material through the solution of the stress field.

Consider a non-homogeneous material containing N isotropic constituents with volume and shear moduli K_r and G_r and a linear coefficient of thermal expansion α_r, with r equal to 1 corresponding to the bonded phase. The microstructure of the composite consists of randomly distributed composite spheres, allowing the macroscopic properties of the composite to remain isotropic (i.e., K_{eff}, G_{eff}, and α_{eff})[3].

The equivalent stiffness can be calculated by applying uniform boundary conditions at the outer boundary ($r \rightarrow +\infty$):

$$U_i(S) = \varepsilon_{ij}^0 x_j \tag{1}$$

where U_i is the displacement field; S is the outer boundary of the composite aggregate; ε_{ij}^0 is the constrained strain tensor; and x_j is the Cartesian coordinate system. The strain tensor is either the spherical tensor $\varepsilon_{ij}^0 = \varepsilon^s \delta_{ij}$ or the bias tensor $\varepsilon_{12}^0 = \varepsilon^d$, and δ_{ij} is Kronecker δ.

The equivalent elastic properties can be expressed as:

$$\begin{cases} K_{\text{eff}} = K_1 + \sum_{r=2}^{N} C_r (K_r - K_1) \dfrac{\langle \varepsilon_{ii}^r \rangle}{3\varepsilon^s} \\ G_{\text{eff}} = G_1 + \sum_{r=2}^{N} C_r (G_r - G_1) \dfrac{\langle \varepsilon_{12}^r \rangle}{3\varepsilon^d} \end{cases} \tag{2}$$

In this formula, C_r is the volume fraction of the r phase; $\langle \varepsilon_{ii}^r \rangle$ and $\langle \varepsilon_{12}^r \rangle$ are the average strains of the aggregate phases under condition Equation (1).

Assuming that the Poisson's ratio of each phase (v_m and v_p) is not temperature dependent, based on the experimental values, the relationship between the bulk modulus of the material, K, and the shear modulus, G, and the Young's modulus, E, and Poisson's ratio, v, can be derived as follows:

$$K = \frac{E}{3(1+2v)} \tag{3}$$

$$G = \frac{E}{2(1+2v)} \tag{4}$$

In predicting the mechanical properties of two-phase composites, the equivalent elastic properties can be determined from the following analytical equations. In the following equations, K is the bulk modulus, G is the shear modulus, E is the elastic modulus, v is the Poisson's ratio, C is the volume fraction, and the subscripts i, m, and eff denote the equivalent properties of the material in the granular phase, matrix phase, and after homogenization, respectively.

The equivalent bulk modulus of elasticity which can be expressed as:

$$K_{\text{eff}} = K_m + \frac{C_i (K_i - K_m)}{1 + \dfrac{(1 - C_i)(K_i - K_m)}{\left(K_m + \frac{4}{3} G_m\right)}} \tag{5}$$

The equivalent shear modulus satisfies the following equality:

$$A\left(\frac{G_{\text{eff}}}{G_m}\right)^2 + B\left(\frac{G_{\text{eff}}}{G_m}\right) + D = 0 \tag{6}$$

where the coefficients A, B and D of the equation are determined by the following equation:

$$A = 8(4-5\nu_m)\left(\frac{G_i}{G_m}-1\right)\eta_1 C_i^{\frac{10}{3}} - 2\left[63\eta_2\left(\frac{G_i}{G_m}-1\right)+2\eta_1\eta_3\right]C_i^{\frac{7}{3}} + 252\left(\frac{G_i}{G_m}-1\right)\eta_2 C_i^{\frac{5}{3}} - 50\left(\frac{G_i}{G_m}-1\right)(7-12\nu_m+8\nu_m^2)\eta_2 C_i + 4(7-10\nu_m)\eta_2\eta_3$$

$$B = -4(1-5\nu_m)\left(\frac{G_i}{G_m}-1\right)\eta_1 C_i^{\frac{10}{3}} + 4\left[63\eta_2\left(\frac{G_i}{G_m}-1\right)+2\eta_1\eta_3\right]C_i^{\frac{7}{3}} - 504\left(\frac{G_i}{G_m}-1\right)\eta_2 C_i^{\frac{5}{3}} + 150\nu_m\left(\frac{G_i}{G_m}-1\right)(3-\nu_m)\eta_2 C_i - 3(7-15\nu_m)\eta_2\eta_3$$

$$D = -4(7-5\nu_m)\left(\frac{G_i}{G_m}-1\right)\eta_1 C_i^{\frac{10}{3}} - 2\left[63\eta_2\left(\frac{G_i}{G_m}-1\right)+2\eta_1\eta_3\right]C_i^{\frac{7}{3}} + 252\left(\frac{G_i}{G_m}-1\right)\eta_2 C_i^{\frac{5}{3}} + 25\left(\frac{G_i}{G_m}-1\right)(\nu_m^2-7)\eta_2 C_i - (7+5\nu_m)\eta_2\eta_3$$

The η_1, η_2 and η_3 in coefficients A, B and D are determined by the following equation:

$$\eta_1 = \frac{G_i}{G_m}(7+5\nu_i)(7-10\nu_m) - (7-10\nu_i)(7+5\nu_m) \tag{7}$$

$$\eta_2 = \frac{G_i}{G_m}(7+5\nu_i) - 4(7-10\nu_i) \tag{8}$$

$$\eta_3 = \frac{G_i}{G_m}(8-10\nu_m) + (7-5\nu_m) \tag{9}$$

Through homogenization of the material phases, microcracks and particle debonding are equated to the pore phase, and changes in the microstructure of the material can be equated to loading injury of the material.

For the composite multi-phase materials, is a composite multi-phase materials in a certain kind of inclusions in the phase stripped out, and then combined with the matrix to become a two-phase hypothetical medium, in the use of two-phase prediction model to calculate the mechanical properties of the hypothetical medium. We are calculating the mechanical properties of an inclusion phase and the porous matrix phase, the volume fraction of the inclusion phase if the whole matrix phase to consider is obviously unreasonable, we can be based on the proportion of different inclusion phase in the whole inclusion phase to allocate the porous matrix phase. Here we assume that the volume of each inclusions phase $z$in the phase composite material is V_Z, $z = 1, 2, 3, \ldots, N$, the volume of the matrix phase is V_j, we calculate the volume fraction of a certain inclusions phase in the whole inclusions phase $n = 0, 1, \ldots, N$, after the matrix phase in accordance with the $X_{1,2,\ldots,N}$assigned to the corresponding inclusions phase, assuming that the two-phase composites in the volume fraction of inclusions phase C_Z can be obtained through the Equation (10):

$$C_Z = \frac{V_Z}{V_Z + V_j X_{1,2,\ldots,N}} \tag{10}$$

We can calculate the mechanical properties of the hypothetical two-phase composites by C_Z respectively, based on which the effective mechanical properties of the phase composites are obtained by weighted averaging the mechanical properties of all its equivalent media according to $X_{1,2,\ldots,N}$ with

the weighted formula:

$$M = \sum_{i=1}^{N} X_i M_i \tag{11}$$

In the Equation (11), M_i is the mechanical property (E or v)) of the hypothetical two-phase medium, i.e., the effective mechanical property of the phase composite material. Knowing the properties of the composite material can be based on $E(\sigma) = \mathrm{d}\sigma/\mathrm{d}\varepsilon$ using incremental theory, can be deduced $\sigma - \varepsilon$ correspondence as Equation (12):

$$\frac{\sigma_{n+1} - \sigma_n}{\varepsilon_{n+1} - \varepsilon_n} = E_n, n = 0, 1, \cdots, N \tag{12}$$

A schematic diagram of multiphase composite material prediction is shown in **Figure 1**, which also shows that when two of the material properties of the particle phase, matrix phase and monolithic material of a certain material are known, the prediction of the other unknown property can be made.

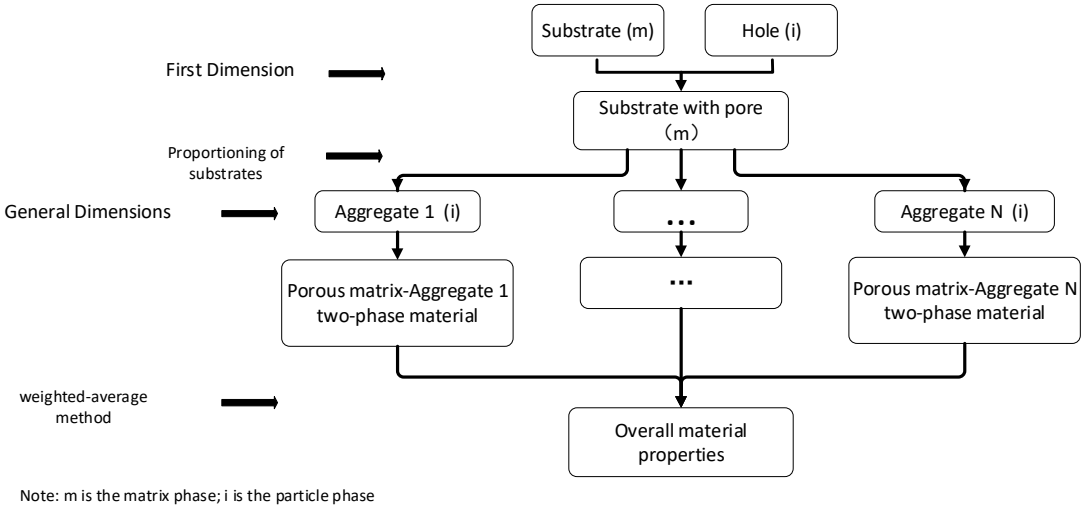

Figure 1. Schematic diagram of multi-phase composite material prediction.

2.2. Mechanical behavior simulation

The interior of the composite material can be regarded as composed of matrix, aggregate and porosity, and there are also high-density microscopic cracks, which can also be regarded as porosity phase. The essence of material stress-strain simulation is that when the material is subjected to tensile stress and compressive stress, the changes among the matrix phase, aggregate phase and porosity phase inside the material are reasonably considered. Multi-step homogenization[6] can transform the changes of each phase in the material into a mathematical model.

Taking the state of the material under pressure as an example, it can be divided into three stages. In the first stage, the internal tangential stress σ_T is less than the damage threshold σ_{mc} of the matrix phase, at which time there is no crack inside the material and the overall mechanical properties of the material are less affected. In the second stage, when $\sigma_T \geq \sigma_{mc}$, due to the difference in mechanical strength between matrix and aggregate, cracks begin to appear at the interface between matrix phase and particle phase, and the overall mechanical properties of the material begin to decline sharply. In the third stage, when $\sigma_T > \sigma_{\max}$, $\sigma_{\max}$ is the ultimate stress of the material, and the mechanical properties of the material are completely destroyed.

According to relevant mechanical behavior studies[8], when the second stage occurs, σ_{mc} corresponds to the maximum elastic strain ε_{emax} of the material. After the material enters the second stage, the strain ε_x at a point is composed of the maximum elastic deformation ε_{emax} and the inelastic deformation ε_i, i.e.,

$$\varepsilon_x = \varepsilon_{\text{emax}} + \varepsilon_i \tag{13}$$

Hild et al.[9] proposed the following relationship between permanent residual deformation ε_p and inelastic deformation ε_i:

$$\varepsilon_i = 2\varepsilon_p \tag{14}$$

The external load at the maximum elastic strain can be obtained from the above formula, and the damage threshold σ_{mc} of the matrix phase can be obtained from the analytical method of elastic mechanics. When $\sigma < \sigma_{mc}$, the stress-strain of the material is in a linear stage, and the mechanical properties of the material are not affected. When $\sigma > \sigma_{mc}$, cracks begin to appear at the interface between the matrix and the particles, and the mechanical properties of the material begin to decrease. According to equation (12), $E(\sigma) = \mathrm{d}\sigma/\mathrm{d}\varepsilon$. By using incremental theory, it can be inferred that $\sigma - \varepsilon$.

3. Prediction of elastic modulus properties of refractories

In this study, the author selected three different types of refractories, which are aluminum-magnesium-carbon refractories[10], magnesium-carbon refractories[11] and aluminum-titanium refractories[12]. These materials represent a variety of inclusion materials, low matrix high aggregate materials and aluminum matrix materials, respectively. The local properties of the matrix phase and inclusion phase required above are listed in **Table 1**.

Table 1. Localized properties of selected materials.

Materials	$E(GPa)$	v	Materials	$E(GPa)$	v
Al_2O_3	380	0.26	$Carbon$	5	0.12
Al	76	0.33	$Resin$	3	0.3
MgO	200	0.25	$Pitch$	1.5	0.3
Fe_2O_3	130	0.3	$Sintered\ magnesia$	150	0.24
$Mullite$	160	0.28	Ti_3AlC_2	297	0.25
$Pore$	-	-	Al_3Ti	216	0.3

3.1. Aluminum-magnesium carbon refractory

In this study, aluminum-magnesia carbonaceous refractory is the representative of multi-inclusion phase. According to the different internal components, the properties of three aluminum-magnesia carbonaceous materials are predicted here. The volume fraction of each component in the three aluminum-magnesium carbon refractories is shown in **Table 2**, which is named AMC. According to the shown in **Figure 1**, you first need to predict the basic mechanics performance of perforated matrix phase, the AMC materials, carbon and resin board can be as matrix, can also be phase as the matrix phase to consider a combination; In this paper, the traditional two-phase generalized self-consistent model is used to homogenize carbon and resin, and the homogenized binding phase is used as the matrix phase. As for the performance calculation of the binding phase, AMC1 is taken as an example, carbon is taken as the matrix phase and resin is taken as the inclusion phase. In this case, the volume content of resin as the inclusion phase in the hypothetical two-phase medium is 5.2/(5.2 + 1.6) = 76.5%. The mechanical properties of carbon and resin combined phases can be obtained by using the

two-phase generalized self-consistent model.

Next, the binding phase and pores are homogenized to obtain the mechanical properties of the porous matrix phase in the first scale. In the process of treating the binding phase and porosity, the porosity is regarded as inclusion, then the inclusion content is 6.6/(6.6 + 5.2 + 1.6) = 49.3%, and the elastic modulus and Poisson's ratio of porous matrix in AMC1 are calculated to be 1.05 GPa and 0.26. The properties of matrix and porous matrix calculated by the three AMC materials are listed in **Table 3**.

Table 3 shows the simulation results of the three AMC materials in the first scale. It can be observed from the results that the porosity is negatively correlated with the mechanical properties of porous matrix in the first scale simulation, which is consistent with the actual situation.

According to the overall scale, the porous matrix phase and other inclusions were homogenized respectively. It should be noted here that the C_Z value needs to be calculated according to Equation (10) in order to allocate matrix phases according to inclusions with different volume fractions, otherwise there will be repeated homogenization of porous matrix phases and inclusions, resulting in a smaller overall material prediction result than the experimental results. The calculated prediction results of porous matrix phase and inclusion phase are listed in **Table 4**. According to the volume fraction of each component in **Table 2**, the relative volume fraction of a certain inclusion in the whole inclusion is calculated, and the actual volume fraction and relative volume fraction of the inclusion are listed in **Table 5**.

Finally, by using the weighted average method to substitute the mechanical properties M_i of the hypothetical two-phase media from **Table 4** and the relative volume fractions $X_{1,2,\ldots,N}$ from **Table 5** into Equation (11), the predicted values of the mechanical properties of the overall composite material AMC are obtained. The predicted values are compared with the experimental values and listed in **Table 6**. It can be observed that the predicted values of the model are within the range of experimental fluctuations, except for a deviation of approximately 30% for the AMC1 material. Upon comparing this material with the other two components, it is found that AMC1 has a higher proportion of aggregate phase and a lower proportion of matrix phase and void phase. This macroscopically manifests as a denser material. Considering the applicability of the model itself, the characteristics of the AMC1 material are closer to those of materials with a low matrix and high aggregate content, for which the generalized self-consistent model is not well-suited. Therefore, a certain deviation is observed in the prediction of the mechanical properties for the AMC1 material.

Table 2. Volume fraction % of each phase of AMC material.

Component	AMC1	AMC2	AMC3
Al_2O_3	78.6	53.3	66.2
Al	1.3	1.3	1.5
MgO	5.2	24.9	6.4
Fe_2O_3	1.5	1.9	1.9
$Mullite$	-	-	8.1
$Carbon$	1.6	3.2	2.8
$Resin$	5.2	5.2	4.6
$Pore$	6.6	10.2	8.5

Table 3. Predicted performance of matrices and perforated matrices.

	Substrate			**Matrix with pores**		
	AMC1	**AMC2**	**AMC3**	**AMC1**	**AMC2**	**AMC3**
E	3.43	3.70	3.67	1.05	0.95	0.99
v	0.26	0.24	0.24	0.26	0.26	0.25

Table 4. Predicted values of hypothetical medium properties of AMC materials.

	Elastic modulus			**Poisson's ratio**		
Materials	**AMC1**	**AMC2**	**AMC3**	**AMC1**	**AMC2**	**AMC3**
Matrix with pores—Al_2O_3	16.34	12.27	10.5	0.19	0.19	0.19
Matrix with pores—Al	13.73	9.30	9.27	0.22	0.21	0.21
Matrix with pores—MgO	15.67	10.04	10.14	0.19	0.19	0.19
Matrix with pores—Fe_2O_3	15.19	9.94	9.68	0.20	0.20	0.20
Matrix with pores—$Mullite$	-	-	10.01	-	-	0.19

Table 5. Actual and relative volume fractions of each inclusions phase of AMC.

	Actual volume fraction (%)			**Relative volume fraction (%)**		
Materials	**AMC1**	**AMC2**	**AMC3**	**AMC1**	**AMC2**	**AMC3**
Al_2O_3	78.6	53.3	66.2	90.8	65.5	78.7
Al	1.3	1.3	1.5	1.5	1.6	1.8
MgO	5.2	24.9	6.4	6	30.6	7.6
Fe_2O_3	1.5	1.9	1.9	1.7	2.3	2.3
$Mullite$	-	-	8.1	-	-	9.6

Table 6. Experimental and predicted values of AMC material properties.

	Experimental values	**Predicted value**
AMC1	23 ± 10	16.24
AMC2	11 ± 2	11.48
AMC3	9 ± 2	10.38

Stress-strain simulation of aluminum-magnesium carbonaceous materials

In the case of AMC1 material, the results of the multistep homogenization calculation in the pressurized state are listed in **Table 7**. According to the existing theory, the fracture strength of the composite is $E/7$. Based on the modified generalized self-consistent model, the elastic modulus of AMC1 was predicted, and the simulation results of the first three iterative steps were analyzed.

The elastic modulus of AMC1 material is 16.24 GPa and the elastic modulus of matrix phase is 3.43 GPa. According to the research of Muñoz et al.[10], it is known that the permanent residual deformation of AMC1 material is $\varepsilon_p = 1.2 \times 10^{-3}$, and the macroscopic failure load is 53 MPa. Combined with Equations (13) and (14), the maximum elastic strain $\varepsilon_{emax} = 1.8 \times 10^{-3}$ of the material can be obtained, and the damage threshold $\sigma_{mc} = 31.29$ MPa of the matrix phase can be obtained by using the elastic analysis method. The other two material parameters are listed in **Table 8**.

Table 7. Elastic properties of the phases of aluminum carbonaceous in compression.

Iteration steps	Matrix volume fraction	Pore volume fraction	Pore volume fraction in the first scale	Modulus of elasticity of a porous matrix at the first scale	Volume fraction of inclusions in the overall scale	Matrix with pores—Al_2O_3 (E)	Matrix with pores—Al (E)	Matrix with pores—MgO (E)	Matrix with pores—Fe_2O_3 (E)	Modulus of elasticity of the material after overall scale weighting
0	6.80	6.60	49.25	1.05	86.6	16.34	13.73	15.67	15.19	16.24
1	6.12	7.28	54.33	0.89	86.6	14.09	12.88	13.57	13.04	13.29
2	5.44	7.96	59.40	0.75	86.6	11.95	10.47	11.58	11.19	11.27
3	4.76	8.64	64.48	0.62	86.6	10.00	8.94	9.71	9.46	9.43
4	4.08	9.32	69.55	0.50	86.6	8.16	7.43	7.98	7.84	7.70
5	3.40	10.00	74.63	0.39	86.6	6.44	5.98	6.33	6.21	6.08
6	2.72	10.68	79.70	0.30	86.6	5.01	4.72	4.94	4.86	4.73
7	2.04	11.36	84.78	0.21	86.6	3.54	3.40	3.51	3.47	3.34
8	1.36	12.04	89.86	0.13	86.6	2.22	2.16	2.20	2.19	2.09
9	0.68	12.72	94.93	0.06	86.6	1.03	1.02	1.03	1.03	0.97
10	0	13.40	100	0	86.6	0	0	0	0	0

Table 8. Matrix phase damage threshold and failure load of AMC material.

	Damage threshold (MPa)	Failure load (MPa)
AMC1	31.29	53
AMC2	21.70	27
AMC3	33.64	48

Based on the calculation results from **Table 8** and in conjunction with Equation (13), the stress-strain curve of the AMC material can be simulated as shown in **Figure 2**. It can be observed that for the aluminum-magnesium-carbon composite material with a higher content of inclusions, the simulated stress-strain curve closely matches the experimental values, with a maximum error of no more than 10%. Overall, the predicted curve tends to be slightly lower than the experimental values. This can be attributed to the influence of various factors such as the composition and fabrication process of the composite material, which may introduce some differences in the overall predictions. During the elastic stage of the stress-strain curve, there is a certain error in the linear portion due to different predicted values of the elastic modulus. In this model, when characterizing the material under compression, the generation of cracks at the interface between particles and matrix is equivalently represented as a conversion from matrix phase to void phase. However, the rate of this void conversion may be faster than the actual situation, resulting in slightly lower overall predicted values compared to the experimental values. Nevertheless, the errors for these three materials are within an acceptable range, and the predicted values show consistent stress levels with the experimental values at the same strain. This indicates that the improved Generalized Self-Consistent Model is feasible for predicting the mechanical properties of such complex composite materials and can provide an initial estimation of their mechanical performance.

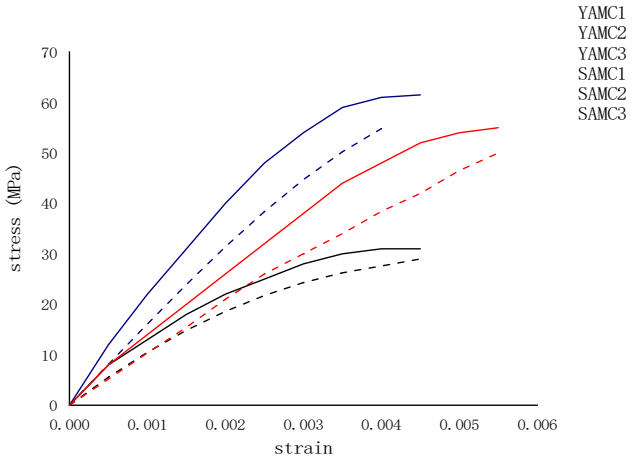

Figure 2. AMC Stress-strain prediction curve YAMC and experimental curve SAMC.

3.2. Magnesia carbon refractory

The magnesium-carbonaceous materials selected in this study have a higher proportion of inclusion in their components than the materials studied so far. **Table 9** shows the volume fraction of the internal components of three magnesia carbon refractories. The mass fraction of each component used in the original data is the mass fraction of each component. According to the principle of generalized self-consistent model, this study has obtained the integral number of each component according to the conversion relationship of the data, and carried out normalization processing, and named the material *M*.

Table 9. Magnesium-carbon refractories % volume fraction of each phase.

Component	M1	M2	M3
Sintered magnesia	87.3	87.7	88.2
Al	2.8	2.8	-
Pitch	5.2	4.2	-
Resin	-	-	6.1
Pore	4.7	5.3	5.7

Similarly, the basic mechanical properties of the porous matrix phase were predicted by homogenizing the matrix phase and the stomatal phase. The elastic modulus of the porous matrix phase of *M*1, *M*2 and *M*3 were 0.48, 0.37 and 0.94, respectively. Then, according to the general scale in the principle, the mechanical properties of porous matrix phase and inclusion phase are predicted by the generalized self-consistent model, and the predicted values are listed in **Table 10**.

Table 10. Predicted values of hypothetical medium properties of magnesium-carbonaceous materials.

	Elastic modulus			Poisson's ratio		
Materials	***M*1**	***M*2**	***M*3**	***M*1**	***M*2**	***M*3**
Matrix with pores—*Sintered magnesia*	10.3	7.5	15.9	0.20	0.21	0.20
Matrix with pores—*Al*	9.6	7.98	-	0.21	0.21	-

The overall elastic modulus of the composite material was determined based on the relative volume fractions of the inclusion phase. The predicted values and experimental values were listed in **Table 11**, where the experimental values were obtained from uniaxial compression tests conducted

using a servo-hydraulic testing machine at room temperature, as recorded in the literature. The results showed that the generalized self-consistent model (GSCM) is not suitable for this type of material with a low matrix content and a high content of aggregates. The reason is that when the matrix phase is relatively low, it cannot effectively encapsulate the aggregates, resulting in a lower overall density and an uneven distribution of structural strength within the material. This non-uniformity significantly affects the overall performance of the material under stress, leading to mechanical instability. For such materials, the GSCM typically assumes an ideal state where the matrix phase adequately surrounds the aggregates, and the components are uniformly distributed. However, in reality, due to the differences in volume fractions between the matrix and aggregate phases, the overall material cannot achieve the envisioned ideal state. The current GSCM model does not effectively consider these factors, hence its poor performance for such materials. The predicted elastic modulus of material M differed significantly from the experimental value; therefore, simulating the stress-strain curve for this material is not appropriate in this case.

Table 11. Experimental and predicted values of magnesium-carbon refractory properties.

	Experimental values	**Predicted value**
***M*1**	4.0	10.3
***M*2**	5.1	7.5
***M*3**	27.0	15.9

The results show that the generalized self-consistent model is not suitable for the material with low matrix and high aggregate. The reason is that when the internal matrix of the material is relatively small, the matrix cannot wrap the aggregate well, resulting in the overall density of the material is low, and the structural strength distribution is not uniform. This non-uniformity will cause the overall properties of the material to be greatly affected when subjected to stress, making the mechanical properties unstable. For this kind of material, the generalized self-consistent model usually assumes that the material is in an ideal state, the matrix can surround the aggregate well, and the internal components are evenly distributed, but in reality, the overall material of this kind of material cannot reach the ideal state because of the difference in the volume fraction of the matrix phase and the aggregate phase. At present, generalized self-consistent models do not take these factors into account well, so they do not perform well for such materials. The predicted elastic modulus of *M* material differs greatly from the experimental value, so the stress-strain curve of this material is not simulated here.

3.3. Aluminum-titanium refractory

The material uses aluminum-titanium carbide as the matrix phase, and the aluminum-titanium carbide of three different materials already contains pores, so the aluminum-titanium carbide can be treated as the matrix phase with pores. The integral number of the three aluminum-titanium refractories for each group is shown in **Table 12**, and they are named *T*1, *T*2 and *T*3 respectively.

Using Al Ti carbide as porous matrix phase, its elastic modulus and Poisson's ratio are 297 GPa and 0.25, respectively, and using Al Ti alloy and Al as inclusion phases, the properties of porous matrix and inclusion are calculated using the traditional two-phase generalized self-consistent model, and the results are listed in **Table 13**.

The performance of the composite material with voids and various inclusions was simulated based

on **Table 13**. Using the relative volume fractions of the inclusions, a weighted average was employed to obtain the predicted values for the overall material. **Table 14** presents a comparison between the predicted values and the experimental values for the overall material. The results indicate that the maximum error between the predicted values and the experimental values for the three materials is 3.8%. This demonstrates that the model can accurately predict the elastic modulus and Poisson's ratio of this type of aluminum-based material. Therefore, the model is capable of predicting the performance of such aluminum-based materials.

Table 12. Titanium-aluminum refractories volume fraction % of each phase.

Component	***T*1**	***T*2**	***T*3**
Ti_3AlC_2	47	52	62
Al_3Ti	28	19	15
Al	25	29	23

Table 13. Predicted properties of hypothetical media for titanium-aluminum materials.

	Elastic modulus			**Poisson's ratio**		
Materials	***T*1**	***T*2**	***T*3**	***T*1**	***T*2**	***T*3**
Matrix with pores—Al_3Ti	264.3	261.3	279.5	0.27	0.27	0.26
Matrix with pores—Al	195.1	192.4	214.9	0.27	0.27	0.27

Table 14. Experimental and predicted properties of Al-Ti material.

	Experimental values	**Predicted value**
***T*1**	219.1	227.6
***T*2**	217.5	219.7
***T*3**	234.0	240.4

Stress-strain simulation of aluminum-titanium materials

The prediction result here is better, similar to the simulated AMC stress-strain method, through the iterative simulation of the growth process of pores in the material, here to the first three steps of simulation results. Taking material *T*3 as an example, the simulation results under pressure are listed in **Table 15**.

Similarly to section 3.1, under the known permanent residual deformation and macroscopic failure load of the materials, the damage thresholds of the three aluminum-titanium materials can be calculated and listed in **Table 16**. The stress-strain curves of the materials can be deduced by combining Equation (12) as shown in **Figure 3**.

According to the results shown in **Figure 3**, the predicted values exhibit good agreement with the experimental values when the strain is less than 0.0015%, with errors within 5%. However, as the stress approaches σ_{max}, the fit between the predicted and experimental values deteriorates, with an error reaching 25%. Additionally, at the same strain level, the predicted stress values are slightly lower than the experimental values. Similar to AMC materials, the main reason for these discrepancies is that these aluminum-based materials have metallic properties. During the iteration process, when simulating the crack growth at the interface between the simulated matrix phase and particle phase, the simulated porosity growth rate is faster than the actual situation. This leads to a faster descent of the predicted

curve in the yield stage, resulting in an overall lower stress level in the predicted stress-strain curve compared to the experimental values. Overall, the predicted values for the three materials maintain the same order of magnitude as the experimental values at the same strain level. Although the error reaches 25% when the stress reaches its peak, the model remains applicable as a tool for estimating the mechanical properties of these materials.

Table 15. Elastic properties of the phases of titanium-aluminum in compression.

Iteration steps	Matrix volume fraction	Pore volume fraction	Pore volume fraction in the first scale	Modulus of elasticity of a porous matrix at the first scale	Volume fraction of inclusions in the overall scale	Matrix with pores—Al_3Ti (E)	Matrix with pores—Al (E)	Modulus of elasticity of the material after overall scale weighting
0	62	0	0	297.0	38	279.5	214.9	240.4
1	55.8	6.2	10	242.5	38	232.1	162.1	204.4
2	49.6	12.4	20	195.6	38	203.1	139.8	178.1
3	43.4	18.6	30	154.8	38	175.5	119.7	153.5

Table 16. Matrix phase damage threshold and failure load of Al-Ti materials.

	Damage threshold (MPa)	Failure load (MPa)
$T1$	334.5	650
$T2$	277.0	720
$T3$	313.2	740

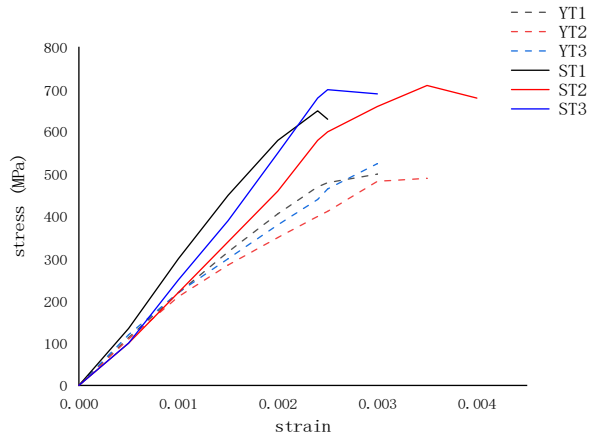

Figure 3. Stress-strain prediction curves YT and experimental ST curves of aluminum-titanium.

4. Results were discussed and analyzed

According to the analysis results, the following conclusions can be drawn:

For more similar to AMC mixed phase materials, mechanical parameters in its composition is known, under the premise of volume fraction and the pore volume, improve the mechanical properties of the generalized self-consistent model for the overall material forecast effect is good, and the stress strain curve simulations and experimental value error value is smaller. As a result, the complexity of mixed types in the material will not affect the prediction effect of the generalized self-consistent model, but compared with the mixed type of simple material, the model of calculation for a long time. For the selected magnesia carbonaceous material, although its composition is relatively simple, a high proportion of aggregate will lead to a decrease in the overall material density. The matrix as a

continuous phase does not enclose the aggregate well, so the strength distribution of the overall material is not uniform. In addition, during the preparation of the material, factors such as formula, temperature and process will have an impact on the strength of the material. For such materials with high aggregate ratio and poor material stability, the generalized self-consistent model is not applicable. At the beginning of the prediction, the model will place the matrix and aggregate in an imaginary medium, in which the two are evenly distributed and the two are wrapped. And the ideal situation for this kind of material, the actual situation is not consistent with it.

As for aluminum-based materials, they have high melting point, high mechanical strength and stable dimensional change characteristics, and the preparation process has little influence on their mechanical properties, and the overall material stability is good. Therefore, good results can be obtained when the generalized self-consistent model is used to predict the elastic modulus of these materials. However, when predicting the stress-strain curve in subsequent iterations, due to the ratio relationship between matrix phase and aggregate phase, the pore conversion rate in the iteration process is too fast, and the difference from the actual situation will cause the predicted value to fail to reach the peak value measured by experiment in the later stage of the curve. In addition, the predicted value of elastic modulus predicted by the model will also affect the fitting degree of the curve.

In summary, this study selected refractories with different characteristics for prediction, and the results show that the improved generalized self-consistent model can still effectively predict AMC materials with complex components, and the iterative stress-strain prediction effect is better. However, for Mg-Carbonaceous materials with high inclusion volume fraction, the prediction effect is not good. In the materials with high inclusion volume, the matrix and aggregate cannot be uniformly distributed, and the ideal state of the generalized self-consistent model is different from that of Mg-Carbonaceous materials. For aluminum-based materials, the predicted value of elastic modulus is in good agreement with the experimental value, but there is an inaccurate situation in the iterative prediction of stress-strain, which is caused by the excessive pore conversion rate in the iterative process, so that the predicted value of stress-strain in the later period cannot reach the expected value.

5. Conclusion

This paper integrates previous research on the generalized self-consistent model and proposes a new approach and hypothesis for material prediction. It also highlights the predictive performance of the model under different material conditions, providing a theoretical basis and new directions for research on the model in the field of composite materials. Through comparative analysis, the study reveals the following findings:

Previous research on the generalized self-consistent model mainly focused on carbon-based materials with matrix volume fractions ranging from 30% to 60% and relatively simple compositions. By applying the model to predict complex multiphase aluminum-magnesium-carbon materials, low matrix-high aggregate magnesium-carbon materials, and aluminum-based materials, it was observed that the predictive performance of the model is influenced by the type, content, and complexity of the matrix. The generalized self-consistent model performs poorly in predicting materials with low matrix content but is effective for materials with complex compositions and aluminum-based materials. In the stress-strain simulation of aluminum-based materials, there is a relatively large error in the later stages. However, this does not affect the applicability of the model in estimating mechanical properties. To reduce the error, it is suggested to incorporate the influence factor of pore generation in the model algorithm for such metal-based materials, ensuring that the simulated pore generation rate is not higher

than the actual rate.

The mechanical properties of composite materials are influenced by many factors. To improve the accuracy and precision of the generalized self-consistent model, it is necessary to consider other influencing factors such as raw material ratios, manufacturing processes, and variations in material composition. These are challenging issues that require the establishment of reasonable influencing factors in the model to enhance its predictive power in material mechanical properties.

Future research can consider introducing more factors and parameters to make the generalized self-consistent model more comprehensive and accurate, thereby improving its predictive ability for complex materials. Furthermore, further exploration of the applicability of the generalized self-consistent model in different material systems and process conditions can expand its scope of application and enhance the reliability of predictions. Additionally, by leveraging existing technologies, it is possible to develop software that utilizes the internal algorithms of the model to predict material mechanical properties. By inputting volume fractions, Young's modulus, and Poisson's ratio of each component, the software can automatically calculate the overall material's mechanical properties. This would enable a preliminary estimation of mechanical properties before material usage, providing an initial assessment of whether the material meets the requirements.

Author contributions

Conceptualization, ZH and ZW; methodology, ZW; software, XL; formal analysis, JL, TZ and DW; writing—original draft preparation, ZH; writing—review and editing, ZW; All authors have read and agreed to the published version of the manuscript.

Conflict of interest

The authors declare no conflict of interest.

References

1. Janto G, Dimitri H, Andreas R. A microcrack-based continuum damage model with application towards refractories. *PAMM* 2016; 16(1).
2. Huang H, Shan ZD, Liu JH, et al. A unified trans-scale mechanical properties prediction method of 3D composites with void defects. *Composite Structures* 2023; 306.
3. Schmitt N, Burr A, Berthaud Y, et al. Micromechanics applied to the thermal shock behavior of refractory ceramics. *Mechanics of Materials* 2002; 34(11).
4. Siboni G, Benveniste Y. micromechanics model for the effective thermomechanical behavior of multiphase composite media. *Mechanics of Materials* 1991; 11(2).
5. Wang ZG, Li N, Kong JY, et al. The mechanical properties of magnesia-carbon refractory matrix were estimated by micromechanical model (Chinese). *Refractory* 2008; (05): 386–388.
6. Liu XM, Wang ZG, Li YR, et al. Simulation of refractory damage process based on multi-scale generalized self-consistent model (Chinese). *Journal of University of Science and Technology Beijing* 2011; 33(04): 468–473.
7. Lurie S, Minhat M. Application of generalized self-consistent method to predict effective elastic properties of bristled fiber composites. *Composites Part B* 2014; 61.
8. Yang K, Wang ZG, Liu CM. Study on nonlinear mechanical behavior of refractory under uniaxial compression based on microscopic damage mechanics (Chinese). *Engineering Mechanics* 2014; 31(7): 199–202.
9. Hild F, Burr A, Leckie F A. Matrix cracking and debonding in ceramic-matrix composites. *International Journal of Solids and Structures* 1996; 33(8): 1209–1220.
10. Muñoz V, Pena P, Martínez T, et al. Physical, chemical and thermal characterization of alumina-magnesia-carbon refractories. *Ceramics International* 2014; 40(7).
11. Musante L, Martorello L, Galliano P, et al. Mechanical behavior of MgO–C refractory bricks evaluated by stress-strain curves. *Ceramics International* 2012; 38(5).
12. Wang HJ, Huang ZY, Yi JC, et al. Microstructure and high-temperature mechanical properties of co-

continuous (Ti_3AlC_2 + Al_3Ti)/2024Al composite fabricated by pressureless infiltration. *Ceramics International* 2022; 48(1).